Design of Beam Lines and KEK Beam Lines

Akihiro Maki

KEK

Design of Beam Lines and KEK Beam Lines

1. Introduction

The gross characteristics of the experimental beams are limitted by the maximum energy and intensity of the accelerator where the beams are installed. The parameters of our synchrotron (KEK-PS), that is, maximum energy of 8 to 12 GeV, beam intensity of 10^{12} to 10^{13} ppp and so on, determine the production rates of secondary particles. So the beam design is how to gather these particles effectively, how to separate specific particles, how to focus and so on.

The experimental beams which I would present today are not the finally authorized plans, but plans which are now on the process of more detailed consideration. Since the budget is very severe, all the required beams are not installed at the early stage. It depends very much on the physics what kind of beams must be installed here at first. I would like to recomend here that they will be reconsidered according to future discussions on physics.

Today I will give you, at first, a short review of beam optics and will introduce you some kinds of beam line elements which are now under construction at our laboratory. Next, I will give you some examples of beam design, and I will enclose some important problems which we encounter in the work of beam design.

II Beam Design

II-1 Beam Optics

Now, let us confine ourselves to handle only charged particles for a time. Usually we handle them with electric and magnetic field of special configuration. So the motion of each particle is completely described by the familiar Lorentz equation :

$$\frac{d}{dt}(m\mathbf{V}) = e(\mathbf{E} + \mathbf{V} \times \mathbf{B}) \tag{2.1}$$

According to this equation, it is clear that a magnetic field of 10 KG gives the same force as a electric field of 3×10^6 V/cm to a particle traveling with the light velocity. The practical limit of today's industrial technique for magnetic field produced by ordinary iron magnet and for electric field are, respectively, about 20 KG and 10^5 V/cm. This is the reason why we use magnetic devices in most cases of beam handling. Of course, electric ones are also used in special cases as will be described in the following.

Let us define a coordinate system as shown in Fig. 1.

$\mathbf{s}_0$ is a unit vector, tangential to the central orbit.

$\mathbf{x}_0$ and $\mathbf{y}_0$ are transverse unit vectors perpendicular to $\mathbf{s}_0$.

ρ is a radius of curvature of the central orbit.

In equation (2.1), we will change an indipendent variable from t to s. Then we get scalar equations

$$\begin{aligned} z'' &= \frac{e}{p}\sqrt{1+z'^2+x'^2}\left[x'B_s - (1+z'^2)B_x + x'z'B_z\right] \\ x'' &= -\frac{e}{p}\sqrt{1+z'^2+x'^2}\left[z'B_s - (1+x'^2)B_z + x'z'B_x\right] \end{aligned} \tag{2.2}$$

where $x' = \frac{dx}{ds}$ etc. Here we will integrate the equation (2.2) with respect to s after neglecting first derivatives of all coordinates for simplicity. This assumption is right in the most beam lines due to the smallness of solid angle. This integration yields

$$\begin{aligned} Z' &= -\frac{eB_x}{P}1 \\ X' &= \frac{eB_z}{P}1 \end{aligned} \tag{2.3}$$

where 1 is a length of magnetic field.

In the other hand, let us condider a focus action of lens with a focal length f as shown in Fig. 2. To work as a lens, there must be a following relation between a coordinate and its derivative :

$$y' = -\frac{1}{f}y \tag{2.4}$$

From the equations (2.3) and (2.4), if we produce a magnetic field distribution as the integrated field strength is proportional to a coordinate,

$$B1 = \pm\frac{p}{ef}y, \tag{1.5}$$

that magnetic field works as a lens for charged particles.

An example is a quadrupole field as shown in Fig. 3 and discussed in the next sub-section.

II-1-a Quadrupole magnet

It is very combinient to use a matrix formula in the calculation of particle trajectory travelling under the influence of magnetic and electric devices. In this formula the final coordinate and its derivative of a particle after travelling through a beam transport system are represented by a new vector given as a product of a matrix and an initial vector

$$\begin{pmatrix} y \\ y' \end{pmatrix} = T \begin{pmatrix} y_0 \\ y'_0 \end{pmatrix} \tag{2.6}$$

The matrix T represents the influence to the particle motion given by the beam transport system.

The thin lens system shown in Fig. 2 is described in the matrix formula

$$\begin{pmatrix} Z \\ Z' \end{pmatrix} = \begin{pmatrix} 1 & f \\ 0 & 1 \end{pmatrix} \begin{pmatrix} 1 & 0 \\ -\frac{1}{f} & 1 \end{pmatrix} \begin{pmatrix} Z_0 \\ 0 \end{pmatrix} = \begin{pmatrix} 1 & f \\ 0 & 1 \end{pmatrix} \begin{pmatrix} Z_0 \\ -\frac{Z_0}{f} \end{pmatrix} = \begin{pmatrix} 0 \\ -\frac{Z_0}{f} \end{pmatrix} \tag{2.7}$$

The right-hand side matrix represents a thin lens of focal length f and the left-hand side matrix does a drift space of length f. So the (1, 2) element of the matrix represents a length of drift space and (2, 1) element does a iniverse of focal length.

Considering in the same way, the matrix for a thick lens, that is, a real quadrupole magnet, is

$$\begin{pmatrix} \cos\varphi & \frac{1}{\sqrt{k}}\sin\varphi \\ -\sqrt{k}\sin\varphi & \cos\varphi \end{pmatrix} \quad \text{in the focal plane}$$

and

$$\begin{pmatrix} \cosh\varphi & \frac{1}{\sqrt{k}}\sinh\varphi \\ -\sqrt{k}\sinh\varphi & \cosh\varphi \end{pmatrix} \quad \text{in the defocal plane}$$

where $\varphi = l\sqrt{k} > 0$ (2.8)

$$k\ [m^{-2}] = 3\frac{g}{p}\frac{[kG/cm]}{[GeV/c]}$$

As you can see easily in the equation (2.8), a real quadrupole magnet does not work only as a pure lens, but also as a drift space of length $\frac{1}{\sqrt{k}}\sin\varphi$ or $\frac{1}{\sqrt{k}}\sinh\varphi$.

Quadrupole magnets are frequently used as a doublet or a triplet, like a lens system of the geometrical optics we often meet in a camera. A quadrupole doublet is composed of a pair of a focus and a defocus lenses as shown in Fig. 4. Today we will confine us only to give you simple and combinient relations among the optical and the geometrical parameters

$$|f_1| = [D\ (D+E)]^{1/2} \tag{2.9}$$

$$|f_2| = DE/f_1$$

$$f_2/f_1 = E/(D+E)$$

From these equations, it may be reminded that the lens near to the image point needs stronger field gradient than the another one, and that the effective focal lengthes of the doublet in the two perpendicular planes are very much different, so it sometimes creates a very deformed image.

To overcome this defect of the doublet, a triplet is sometimes used. But triplet has other defect comparing with the doublet. Triplet requires a larger g·l value and a larger cost for the same effective focal length and the same beam momentum.

II−1−b Bending Magnet

The bending magnets used as a beam line elements, in most cases, satisfy the symmetry equations

$$B_y(y) = B_y(-y) \quad B_x(y) = -B_x(-y) \quad B_s(y) = -B_s(-y) \tag{2.10}$$

Then the equations of motion are obtained in the linear approximation

$$\begin{aligned} &z'' + kz = 0 \\ &x'' - (k - \frac{1}{\rho^2})x = -\frac{1}{\rho}\frac{\Delta P}{P_0} \\ &\text{where} \quad k(s) = \frac{e}{\rho_0}\frac{\partial Bz}{\partial x}\Big|_{z=x=0} \end{aligned} \tag{2.11}$$

The radius of curvature, ρ, is given in a convinient form for practical calculation

$$\frac{1}{\rho}(m^{-1}) = 0.03\frac{B}{P}\frac{(kG)}{(GeV/c)} \tag{2.12}$$

The transformation matrix for bending magnet is, in general case, represented as

$$T = \begin{pmatrix} \cos(\theta+\beta_0)/\cos\alpha_0 & \rho\sin(\theta+\alpha_0+\beta_0) \\ -\sin\theta/\rho\cos\alpha_0\cos\beta_0 & \cos(\theta+\alpha_0)/\cos\beta_0 \end{pmatrix} \tag{2.13}$$

in the horizontal plane. Variables are defined in Fig. 5. The figure shows a sector magnet ($\theta \neq 0$). In this case, as you can see easily, this magnet acts as a lens of focal length $f = \rho\cos\alpha_0\cos\beta_0/\sin\theta$.

In the field of high enery physics, they sometimes use rectangular magnets ($\theta = 0$) for flexibility. These magnets have of course no focus action and act only as a drift space of length $\rho\sin\phi$ for a monochromatic beam if they were used in a symmetrical fashion, i.e. $\alpha_0 = \beta_0$

Next I will mention a momentum dispersion in a bending magnet. Today I will confine myself to give you the most simple case, that is, the case of rectangular magnet ($\theta = 0$) used in a symmetric fashion ($\alpha_0 = \beta_0$). Only the first order dispersion will be concerned. Because I think it will give you a sufficient image on the momentum dispersion.

In this case, the central momentum component is transformed with the matrix

$$T_0 = \begin{pmatrix} 1 & \rho\sin 2\alpha_0 \\ 0 & 1 \end{pmatrix} \tag{2.14}$$

as I have shown above. The off-central momentum component which has momentum of $p_0 + \Delta p$ is transformed with the matrix

$$\begin{pmatrix} 1+\Delta\beta_0\tan\alpha_0 & \rho_0\sin 2\alpha_0\left\{1+(\frac{\Delta p}{p_0})+(\Delta\beta_0/\tan 2\alpha_0)\right\} \\ 0 & 1+\Delta\beta_0\tan\alpha_0 \end{pmatrix}$$

$$\text{where} \quad \Delta\beta_0 \simeq -0.03\frac{BL}{p_0\cos\alpha_0}\frac{\Delta p}{p_0} \tag{2.15}$$

Above are all in the horizontal plane. In the vertical plane, the transformation matrix is given by

$$\begin{pmatrix} 1-\varphi\tan\alpha_0 & \rho\varphi \\ \rho^{-1}(\varphi\tan\alpha_0\tan\beta_0-\tan\alpha_0-\tan\beta_0) & 1-\varphi\tan\beta_0 \end{pmatrix} \tag{2.16}$$

II－1－c Separator

There are used many kinds of separators in the world. But today I will explain only on the DC separator which is now under construction at our laboratory. A DC separator is a vacuum chamber in which an anode and a cathode are located. A very strong electric field, from about 50 to 100 kV/cm, is realized in the space between the two electrodes, and bends each particle in the beam by some angle which depends on the velocity of each particle. So we can separate different kinds of particles which has different masses if the momentum of beam is defined with bending magnet and slit system.

Practically we use also a magnetic field perpendicular both to the electric field and the beam direction, and make only wanted particles go straight. Unwanted particles are rejected with the slit located at the next focus. Schematics of DC separator is shown in Fig 6.

We sometimes use a difinition of the separation vector which shows amount of separation between wanted particles and unwanted particles in the phase space. The separation vector is

$$\begin{aligned} S &= (\Delta z, \Delta z') \\ &\simeq \left(-\frac{1}{2}\gamma E1^2, -\gamma E1\right) \end{aligned} \tag{2.17}$$

where $\gamma=\frac{e}{pc}(\beta_u-\beta_w)/\beta_u\beta_w$

$\beta_u=\frac{v}{c}$ of unwanted particle.

You must watch at the fact that the spacial separation Δy is proportional to the electric field strength and to square of the length of the electric field. But the most important fact is that the spacial separation is proportional to the γ-function which is propotional to inverse cube of the momentum at high energy. These facts make the particle separation almost impossible at high energy.

II－2 Beam Design As A System

It is an important purpose for a designer of beam line to get proper intensity, image size or parallelity of beam and so on. Among them beam intensity is the most essential property for experimenters.

Flux of secondary particles is represented as

$$F=\frac{d^2N}{dpd\Omega}\varepsilon It\Delta\Omega\frac{\Delta p}{p}p\exp(-L/L_0) \tag{2.18}$$

where $\frac{d^2N}{dpd\Omega}$ is production rate of secondary particle at the target ; I intensity of primary proton beam ; t target efficiency ; ε transmission factor ; $\Delta\Omega$ solid angle ; $\frac{\Delta p}{p}$ momentum bite ; p central momentum ; exp $(-L/L_0)$ decay factor ; L beam length ; and $L_0=\frac{p}{m}c\tau$ decay length of unstable particle.

Among these parameters, I will explain about some of them.

II−2−a Particle Production Rate

When a high energy accelerator was constructed, the first experiment was secondary beam survey, that is, measurements of production rates of many kinds of secondary particles. Those data are compiled in table I. This is, of course, not a complete list. In the table, the higher energy data than that of Serpukhov are excluded.

We can estimate the production rate for our KEK case from these data. But there are some inconsistencies among them, and these data do not cover all angular and energy region which we need.

On the other hand, some people have tried to describe these data in theoretical and empirical formula. They are ;

1. Cocconi's formula

$$\frac{d^2N}{dpd\Omega} = \frac{n_\pi}{2\pi}\frac{T}{p_o^2}\left(\frac{p}{T}\right)^2 e^{-p/T}\cdot e^{-p\theta/p_o} \tag{2.19}$$

where n_π is mean multiplicity of pion, T mean energy of pion, p laboratory momentum of pions, $2p_o$ mean transverse momentum and θ laboratory production angle of pions.

This formula was used as a stant point by other peoples.

2. Trilling's formula

He assumed that low energy pions were produced by statistical boil-off process and that high energy pions were decay products of isobars produced at forward angle.

$$\frac{d^2\sigma}{dpd\Omega} = A_1 p^2 \exp\left(-A_2\frac{p}{\sqrt{p_i}} - A_3 p\sqrt{p_i}\theta^2\right) + \frac{B_1 p^2}{p_i}\exp\left(-B_2\left(\frac{p}{p_i}\right)^2 - B_3 p\theta\right) \tag{2.20}$$

where p is momentum of secondary particle, p_o momentum of primary proton, θ laboratory angle of secondary particle, and A_1 to A_3, B_1 to B_3 parameters.

4) Ranft's formula

He parametrized all exponents of p, p_i and θ in Cocconi's formula.

$$\frac{d^2N}{dpd\Omega} = A_1 p^{A_2} p_o^{A_3}\exp\left(-B_1 p^{B_2} p_o^{B_3} - C_1 p^{C_2} p_o^{C_3}\theta^{C_4}\right) \tag{2.21}$$

5) Sanford & Wang's formula

They approached not physically but in pure mathematical way, giving attention to the angular dependence and the energy dependence of the forward production rates of the experimental data from 10 to 30 GeV/c.

$$\frac{d^2N}{dpd\Omega} = C_1 p^{C_2}\left(1-\frac{p}{p_o}\right)\exp\left[-\frac{C_3 p^{C_4}}{p_o^{C_5}} - C_6\theta^m\left(p - C_7 p_o\cos^{C_8}\theta\right)\right] \tag{2.22}$$

where C_1 to C_8 and m are parameters and m is practically unity ;

The last formula represents all data the most nicely. From now I will always use this formula when I estimate the production rates at our laboratory.

I will give you some examples of the production rates caluculated with Sanford-Wang's formula. They are given in Figs 7, 8 and 9.

II−2−b Beam Separation

As I mentioned in II−1−c, it is very difficult to separate high energy particles. In principle it may be possible to separate them with longer separator. But longer separator requires longer beam length which increase decay of unstable secondary particles.

I will give you an example of beam separation in Fig 10. It shows the separation between pions and kaons in the KEK-K2 beam which will be explained below. In the left-hand side of the figure, aberrations are are not included and it seems that kaons are nicely separated from pions. But they are hardly separated at momentum of 2.5 GeV/c in the right-hand side where aberrations are concerned. When physical separation is not enough, the transmission factor (ε) must be decreased to yield an enough ratio of wanted particle to unwanted particle.

II−2−c Decay Loss

Most of secondary particles decay in a short time. For example, charged pions, charged kaons and long lived neutral kaons have mean lives of 2.60×10^{-8} sec, 1.24×10^{-8} sec and 5.172×10^{-8} sec, respectively. So their charactristic decay lengthes are, respectively, 7.81 m, 3.70 m and 16.14 m.

Decay factor is given by

$$f_d = \exp(-L/L_o) \tag{2.23}$$

where $L_o = \frac{p}{m} c\tau$. $\frac{p}{m}$ represets relatiristic prolongation. Decay loss is not serious for high momentum particles and also for lighter particles. Then this problem is the most serious in charged kaon beam lines, especially in low momentum kaon beam lines.

I will give a result of short calculation for you to have a rough image in table II.

III KEK Beam Magnets and DC Separator

We have designed some elements for KEK beam lines. You will use these elements in a few years. So I will introduce you them here.

III–1 Bending magnet (8D320)

One of the KEK standard magnets has been designed and is now under construction in the factory. The drawings given in Fig 11 show the bending magnet of 8D320 type. Conductors are winded up in the window frame type. Designed maximum field is 20 KG. Total weight is about 18 tons.

III–2 Quadrupole magnet (Q420)

This magnet is also now under construction in the factory. The drawings are given in Fig 12. It's aperture and length are 20 cmϕ and 100 cm respectively. Designed maximum field gradient is 1 KG/cm. Total weight is about 6 tons.

III–3 Superconducting quadrupole magnet (Super Q)

This is of course not an ordinal quadrupole magnet. This has a iron frame as return path. This is commonly called a Panofsky magnet. This magnet is also now under construction not in the factory but in our laboratory.

Effective aperture is 20 cmϕ. Length is 90 cm. Designed maximum field gradient is 1.5 KG/cm. This magnet is intended to be used as a quadrupole doublet just before the bubble chamber to get a wide and thin parallel beam at the chamber. This will be able to be used as a narrow quadrupole magnet in the beam lines for counter experiments. Fig 13 shows the structure of this magnet.

III–4 DC Separator (SPL301–C)

This separator is a very unique type as shown in Figs. 14 and 15. We call it build-in type separator because the 600 KV power supply is build in the vacuum chamber. This is the first trial in the world. We believe it can be handled very easily.

The internal diameter of the vacuum chamber is 1400 mmϕ and the length is 3000 mm. It becomes a long separator if it was used as a tandem with other chambers. A tarbomolecular pump is installed as a main pump to realize a clean vacuum. This made us free from maintenances for vacuum.

IV KEK Experimental Beams

IV−1 Brief Sketch of the KEK−PS

The maximum energy of the KEK accelerator is 8 GeV at the first stage and will be escalated up to 12 GeV in 1977. The intensity was designed to be 10^{13} ppp at repitition rate of 0.5 pps

This machine is of a quadrant type and so has four straight sections. The first straight section (S1) is for the injection from the booster synchrotron. The fourth straight section (S4) is for the RF acceleration. The remained two straight sections (S2 and S3) are used to extruct proton beams. At the S2 section a short spill beam is ejected for bubble chamber experiments, and a long spill beam for counter experiments is extructed at the S3 section. Details of a short spill beam were described in the KEK Annual Report of 1971. A long spill beam is yet at the stage of study.

IV−2 Secondary Beams

1) K1 Beam

This is a medium energy separated and high energy unseparated beam for bubble chamber experiments. A nuclear target is bombered with a short spill proton beam extructed at the S2 straight section. Secondary beams are separated with two 9−meter−separators in two stages. A doublet of a super conducting quadrupole magnets which was shown in Fig. 13 is to be installed at the last stage of the beam line to realize a thin parallel beam in the bubble chamber. Available beams are charged pions and proton of momentum up to 6 GeV/c, charged kaons and anti-proton up to 4 GeV/c. Energies of kaons and anti-proton are limitted by separation. The arrangement of magnets and separators is shown in Fig 16.

2) K2 beam

This is a medium energy enriched beam for counter experiments. The target position is the focal point in the long spill proton beam extructed at the S3 straight section. There used a 6−meter DC separator. Beam is bended two times to the same direction to get a momentum recombined image at the final focus. Available beams are proton, pions and kaons up to 2.5 GeV/c. The maximum momentum is limitted by the last bending magnet. The arrangement is shown in Fig 17. Beam flux is calculated with Sanford-Wang's empirical formula and shown in Fig 18. There, fluxes are shown for two cases, that is, for the primary protons of 8 GeV and of 12 GeV. The curves for kaons do not include the transmission factors mainly due to the separation. It may be considered to be about 0.1 at the maximum momentum and to be larger at lower momentum.

3) π1 beam

This is a high energy unseparated beam for counter experiments. Maximum momentum is 10 GeV/c. Target is the same one as that of K2 beam. Thus, of these two beams, the another beam of the main user's beam are limitted in the charge selection of the beam and the momentum, because not only the target but also the first bending magnet must be used for the two beams simultaneously.

Beam envelopes are shown in Fig. 19. There some of beam characters are described. Momentum dispersion at the first focus 7.4 mm per $\frac{\Delta p}{p} = 1\%$ and the beam spot size at the final focus is shown in the figure. Beam fluxes are also shown for positive and negative pions. Arrangement of this beam line is shown in Fig 17.

4) N 1 Beam

This is a 3.7° neutral beam for counter experiments. Available beams are long lived neutral kaons and neutrons. Fluxes and energy spectrum are not estimated pricisely. I will show you an example here for reference. Fig 20 shows the flux and the energy spectrum of the Berkeley K_L^0 beam. Energy of primary proton is 6 GeV in this case. In our case, that is 8 or 12 GeV, so more intense and higher momentum beam will be available.

5) T 1 Beam

This is a test beam with momentum of 0.6 GeV/c. Magnets for this beam are now installed in a positron beam line for bubble chamber at INS electron synchrotron. This beam will be used to test many newly constructed counters and chambers, and so on.

6) Other Beams

Other beams are also proposed. For example, a muon beam with momentum up to 4 GeV/c, a O° neutral beam and others are now under consideration.

V Final Remarks

I have explained about some beams which can be realized at our laboratory. I want to recommend here the followings. These plans have not been authorized by any committee and most of these plans are studied to design beam line elements. Therefore some of them will be realized with experimenter's supports and others will be not. Our limitted budget may also suppress some of them even if they got experimenter's supports. But it is the strength of physical requests to decide whicn beam will get the first priority. So we will expect many excellent proposals from you.

On the other hand, a new idea for beam design will make experiments effective and will make new valuable experiments possible. We have now some useful programs for beam design and would prepare more combinient programs. So you can use these programs if you want to design some beams.

REFERENCE

1. K.G. Steffen

High Energy Beam Optics

Interscience Publishers, 1956– 1965

2. N.M. King

Theoretical Techniques of High Energy Beam Design

Progress in Nuclear Physics, vol.9, 1964, p.71

3. K.L. Brown

A First- and Second-Order Matrix Theory for the Design of Beam Transport Systems and Charged Particle Spectrometers

SLAC–75

PROGRAM

1. ASP

Ray Tracing Calculation

To search the most probable magnetic field of quadrupole magnets

2. TRANSPORT

Phase Space Ellips Calculation

To get the most probable values of many beam line parameters

List of Table

Table I Data compilation of production rate of secondary particles

Table II Decay factor for unstable secondary particles

Figure Caption

Fig. 1 Definition of coordinate system (z, x, s)

Fig. 2 Focus action of lens

Fig. 3 Quadrupole magnetic field configuration

Fig. 4 Quadrupole doublet

Fig. 5 Particle deflection in bending magnet

Fig. 6 Schematics of DC separator

Fig. 7 Negative pion production rate calculated with Sanford–Wang's formula

Fig. 8 Positive kaon production rate calculated with Sanford–Wang's formula

Fig. 9 Negative kaon production rate calculated with Sanford–Wang's formula

Fig. 10 Example of beam separation between pion and kaon in the KEK K2 beam

Fig. 11 Drawings of 8D320 bending magnet

Fig. 12 Drawings of Q420 quadrupole magnet

Fig. 13 Drawing of KEK super conducting Panofsky magnet

Fig. 14 Schematics of SPL 301–C DC separator

Fig. 15 Photo of SPL 301–C DC separator

Fig. 16 KEK–K1 beam line

Fig. 17 KEK–K2 and KEK–π1 beam lines

Fig. 18 Flux of secondary particles in K2 beam estimated with Sanford–Wang's formula

Fig. 19 Beam envelopes of KEK–π1 beam

Fig. 20 Energy spectrum of long lived neutral kaon of Berkely 3.7° beam

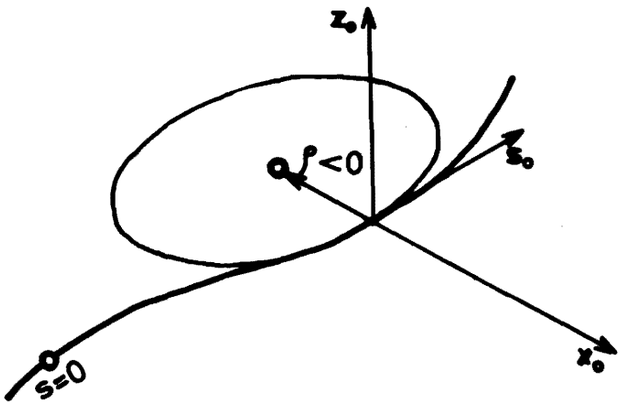

Fig. 1

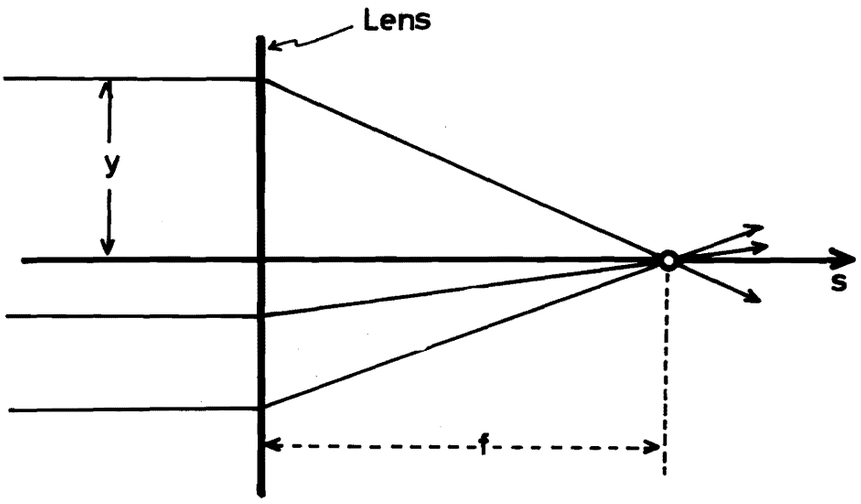

Fig. 2

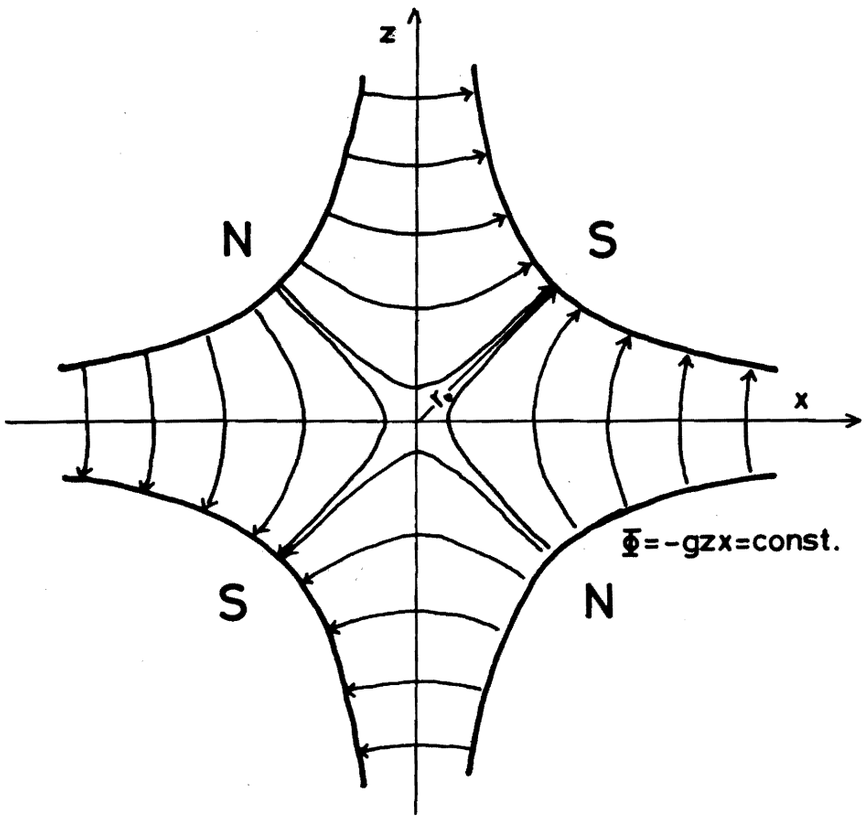
z
N
S
x
Φ=-gzx=const.
S
N

Fig. 3

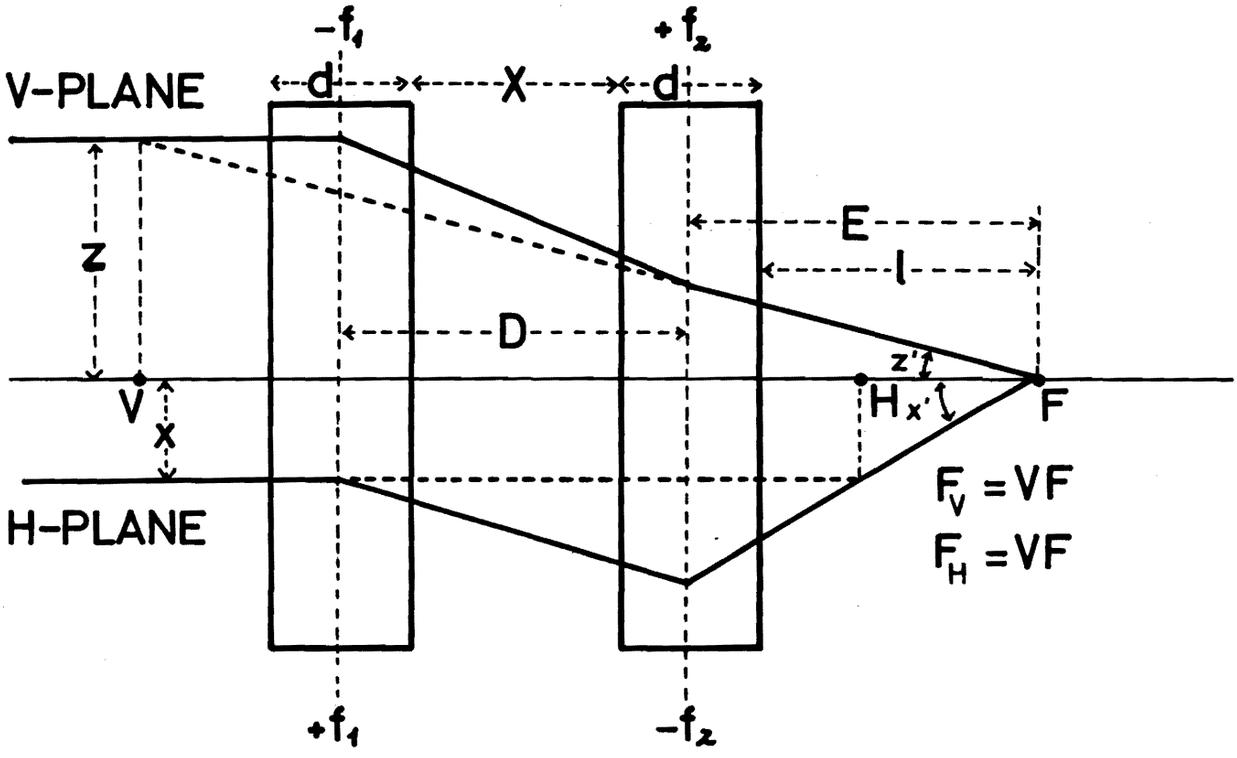
-f1
+f2
V-PLANE
d
X
d
E
l
z
D
z'
V
x
Hx'
F
H-PLANE
FV =VF
FH =VF
+f1
-f2

Fig. 4

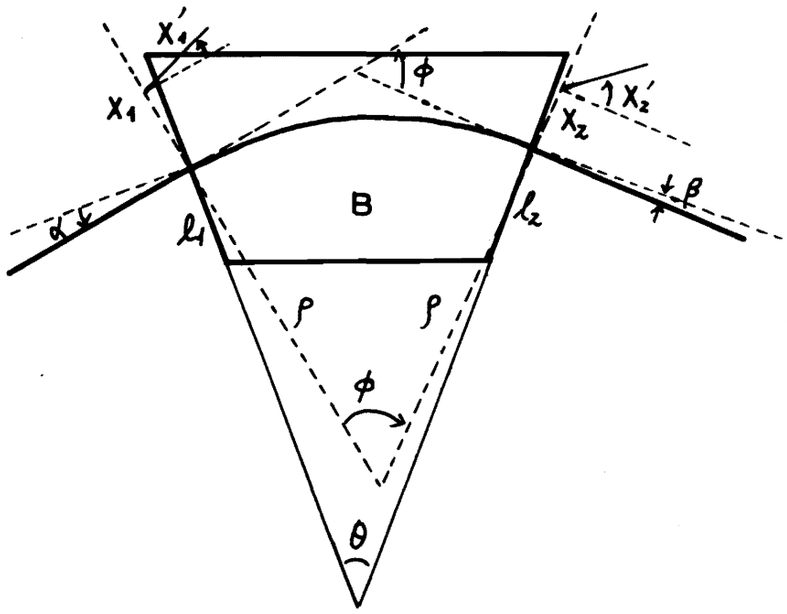

Fig. 5

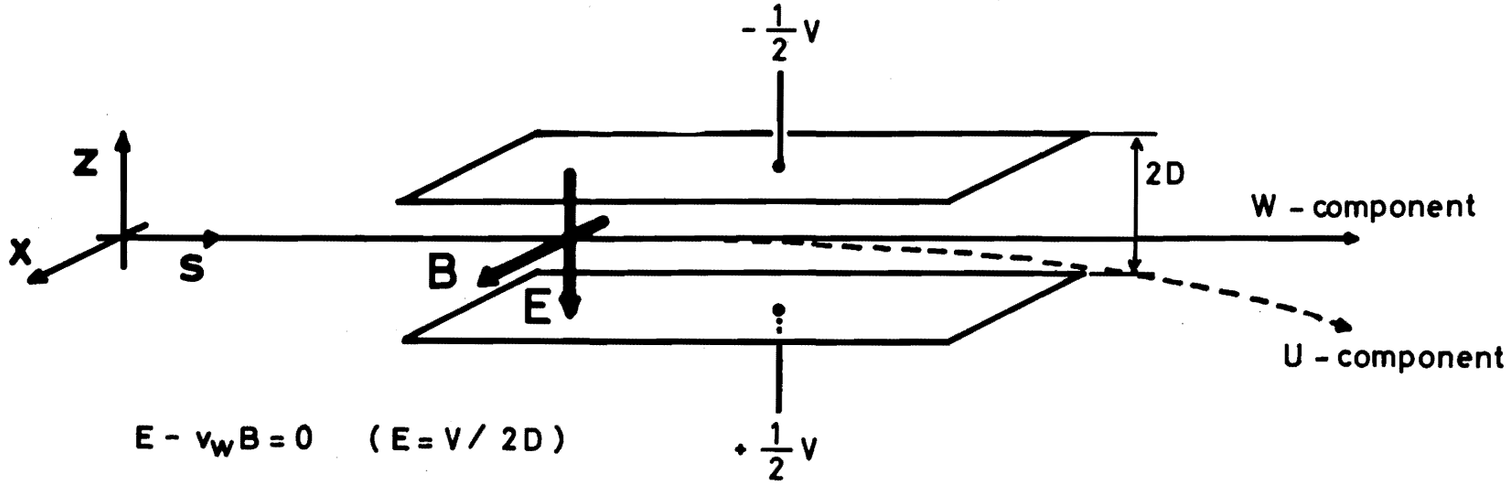
$-\frac{1}{2}V$
Z
X
S
B
E
2D
W - component
U - component
$E - v_W B = 0 \quad (E = V / 2D)$
$+\frac{1}{2}V$

Fig. 6

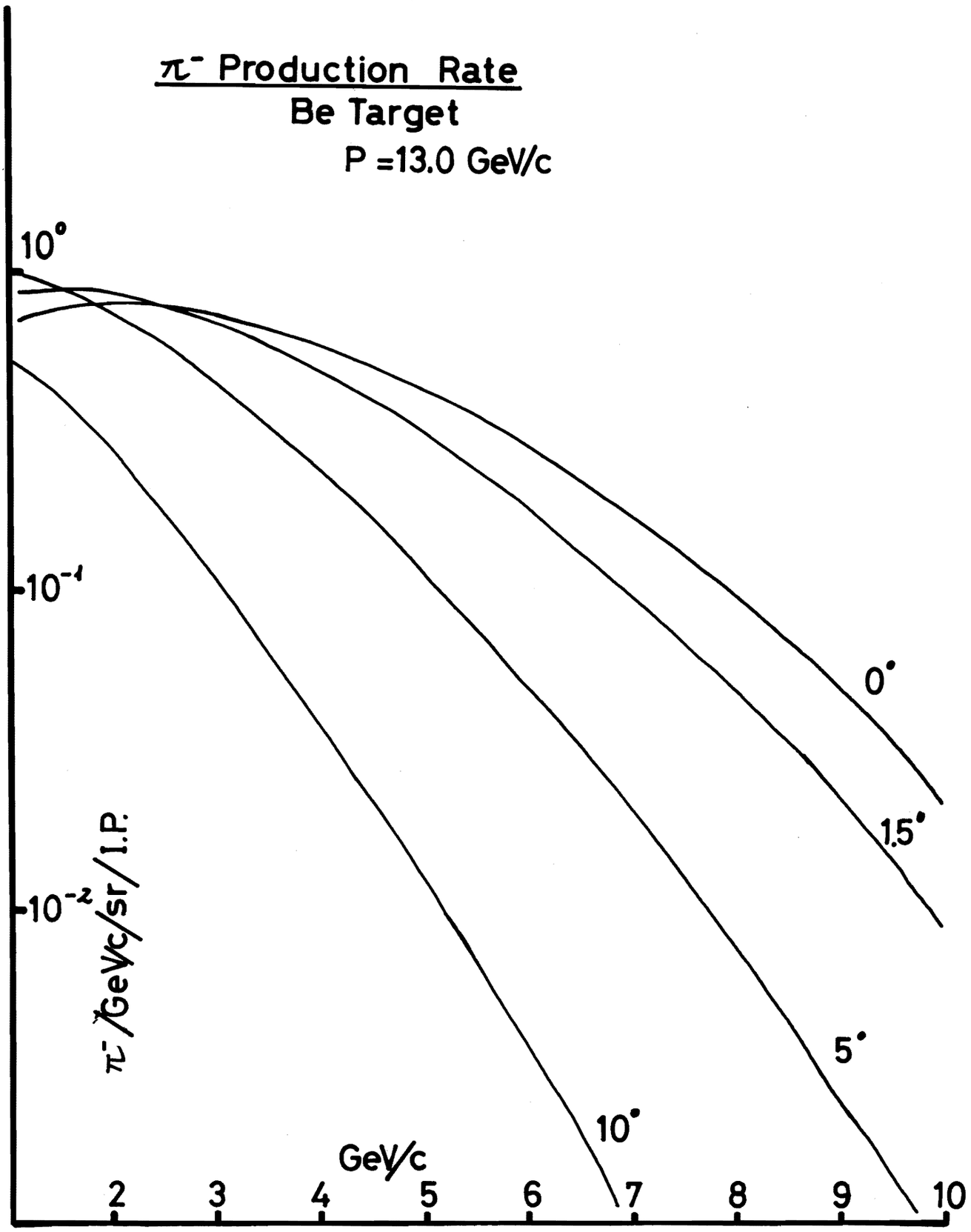
π⁻ Production Rate
Be Target
P =13.0 GeV/c
10°
10⁻¹
10⁻²
π⁻/GeV/c/sr/1.P.
0°
1.5°
5°
10°
GeV/c
2
3
4
5
6
7
8
9
10

Fig. 7

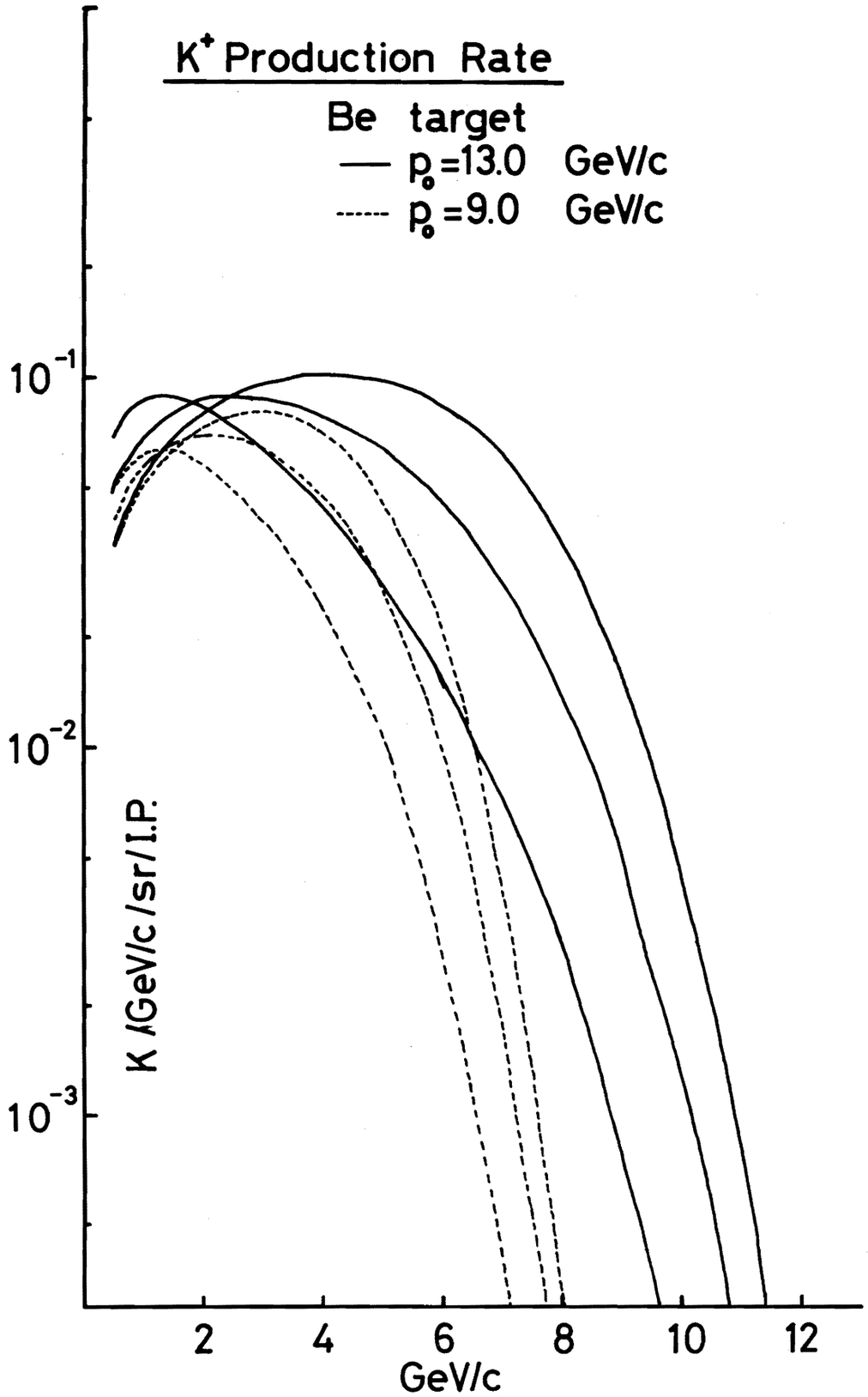
K+ Production Rate
Be target
p0=13.0 GeV/c
p0=9.0 GeV/c
10-1
10-2
10-3
K /GeV/c /sr/ I.P.
2
4
6
8
10
12
GeV/c

Fig. 8

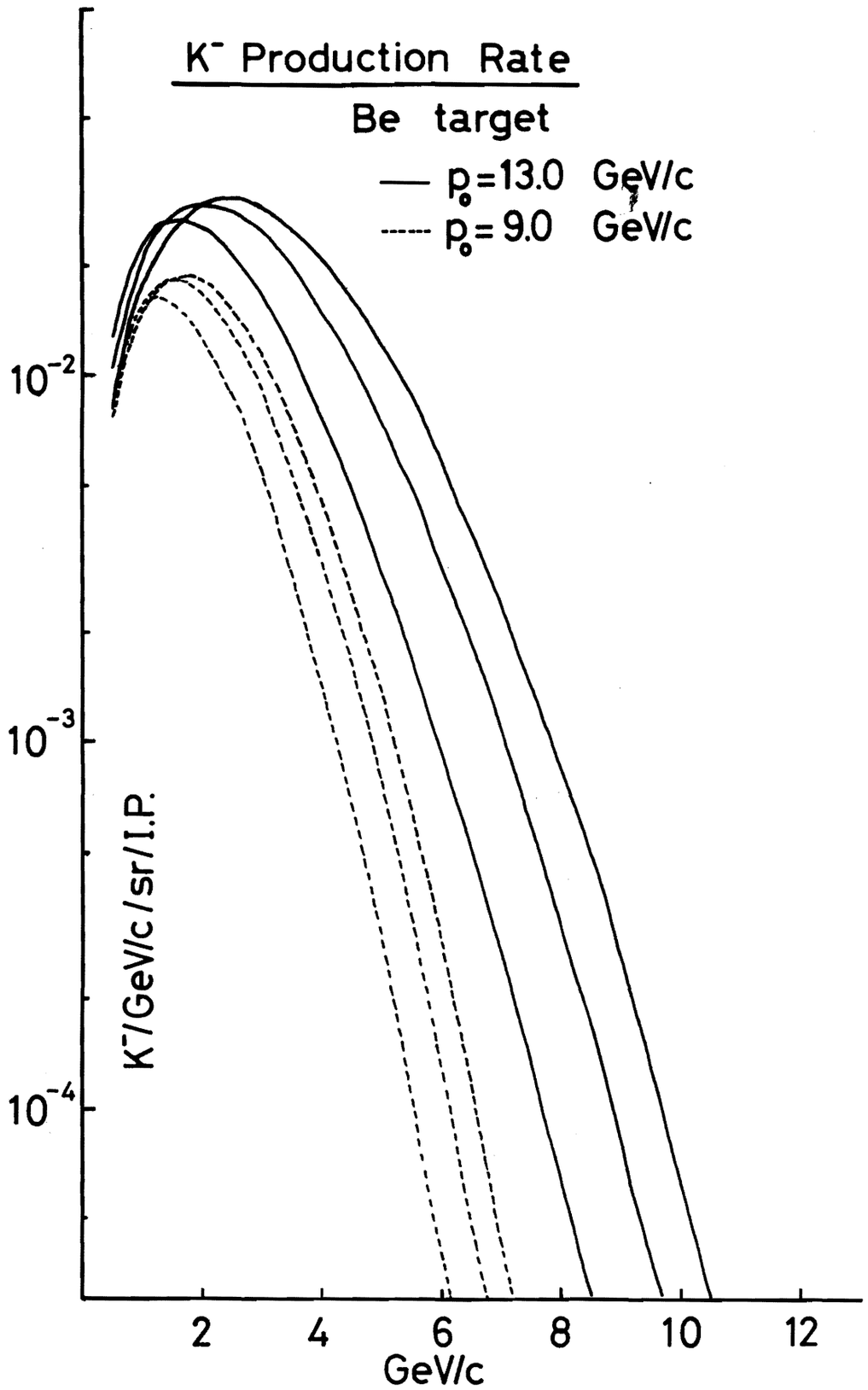
K⁻ Production Rate
Be target
p₀=13.0 GeV/c
p₀= 9.0 GeV/c
10⁻²
10⁻³
10⁻⁴
K⁻/GeV/c/sr/I.P.
2
4
6
8
10
12
GeV/c

Fig. 9

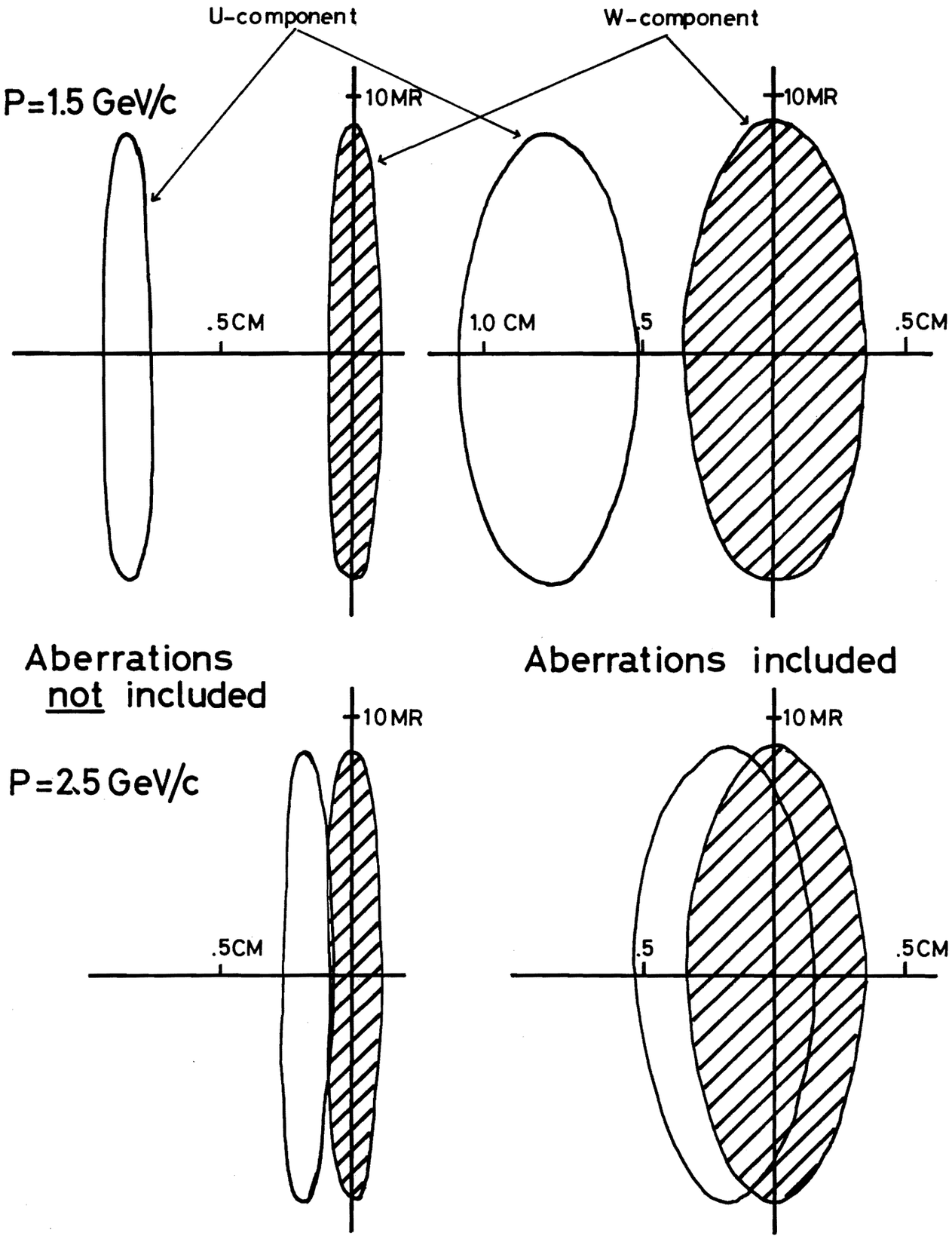
U-component
W-component
P=1.5 GeV/c
10MR
10MR
.5CM
1.0 CM
.5
.5CM
Aberrations
not included
Aberrations included
P=2.5 GeV/c
10MR
10MR
.5CM
.5
.5CM

Fig. 10

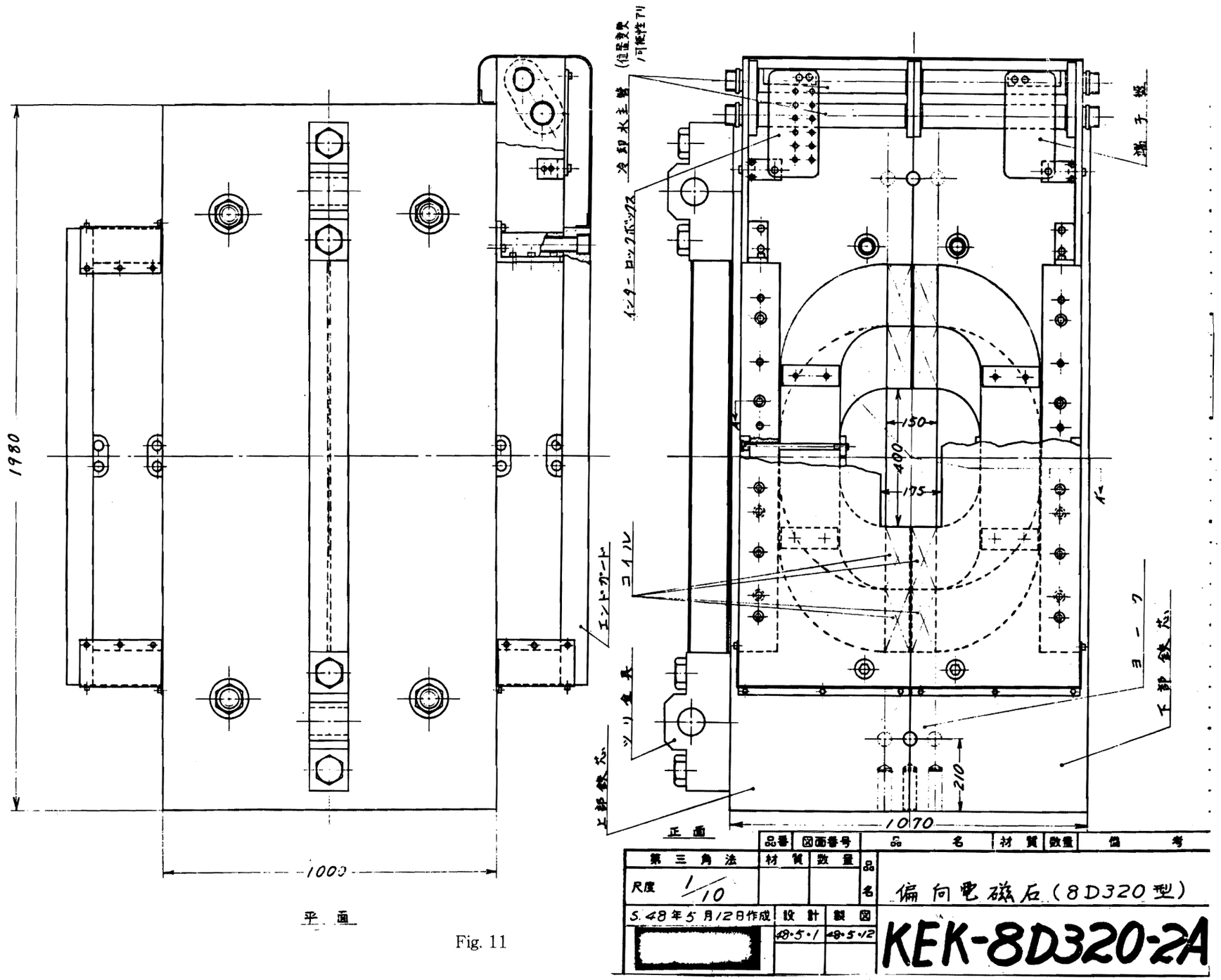
1980
1000
平面
正面
1070
210
400
150
175
コイル
ツリ金具
上部鉄芯
下部鉄芯
端子盤
品番
図面番号
品名
材質
数量
備考
第三角法
尺度 1/10
S.48年5月12日作成
設計
製図
48・5・1
48・5・12
偏向電磁石（8D320型）
KEK-8D320-2A

Fig. 11

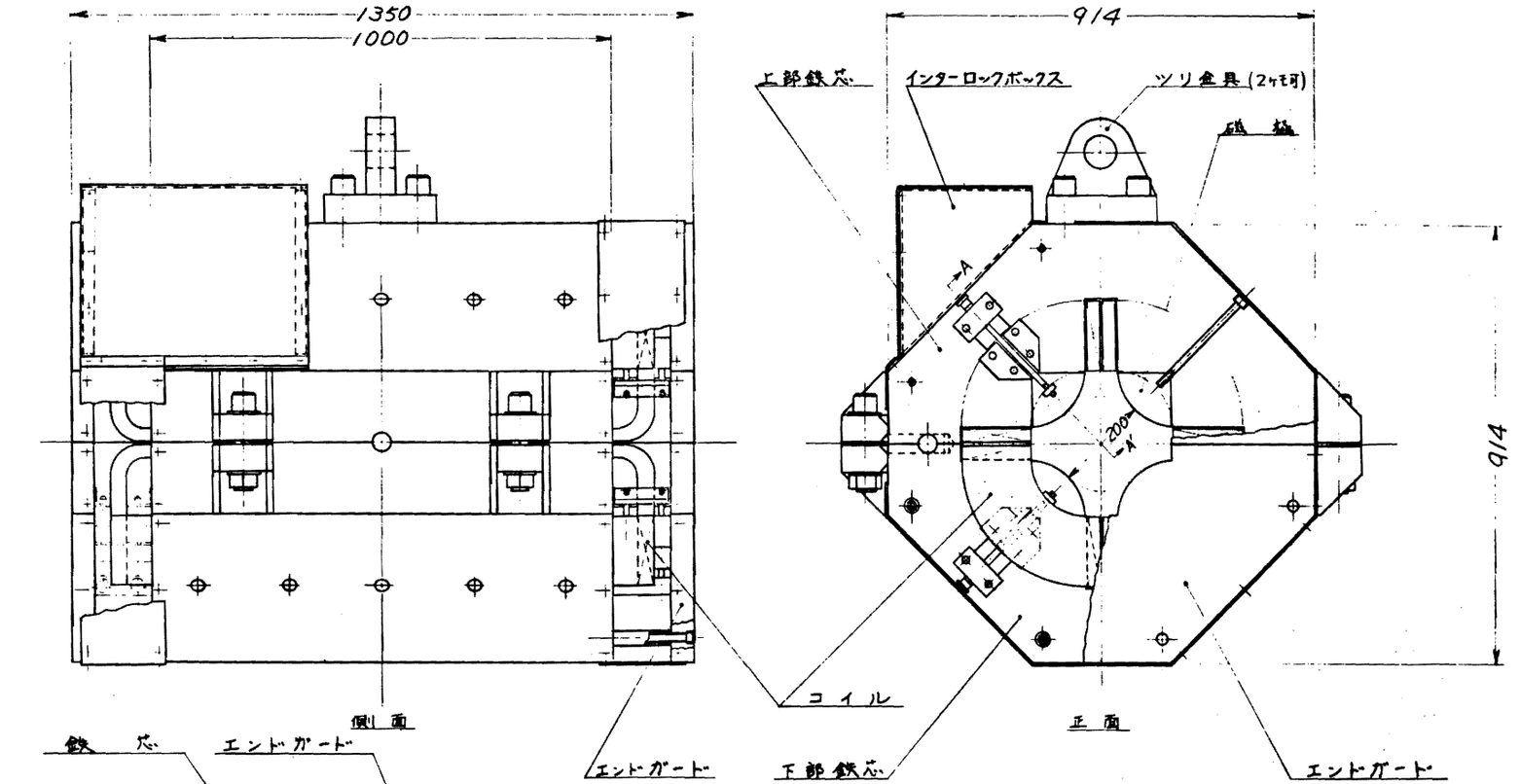

A–A′ 断面

【記】 磁極ノ双曲面仕上ハ見積外トスル。

Fig. 12

	品番	図面番号	品名	材質	数量	備考
第三角法	材質	数量	品名	収斂電磁石 (Q420型)		
尺度 1/10						
S.48年5月21日作成	設計	製図				
	48-5-10	48-5-21				

KEK-Q420-2

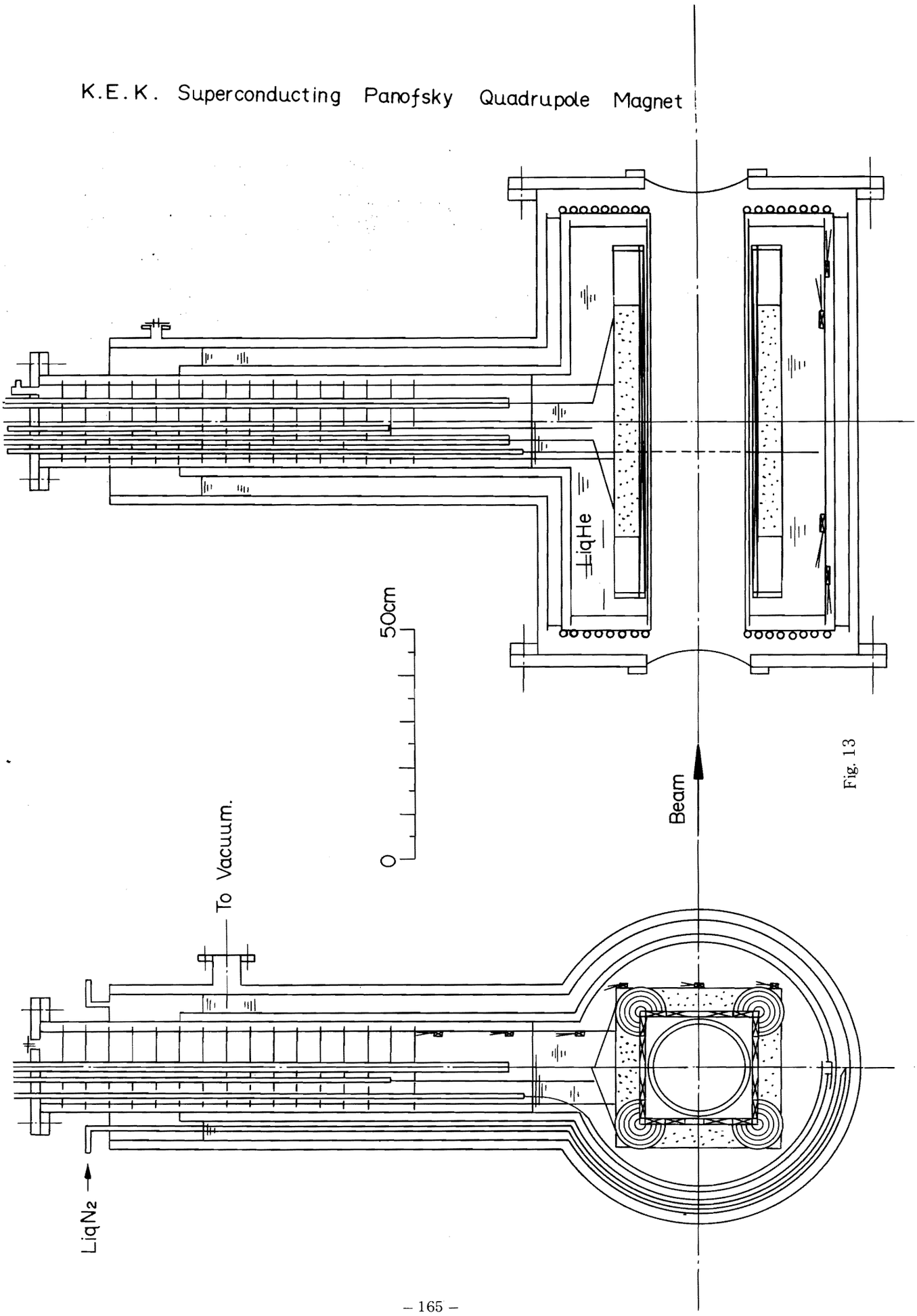
K.E.K. Superconducting Panofsky Quadrupole Magnet
LiqHe
50cm
0
Beam
To Vacuum.
LiqN2

Fig. 13

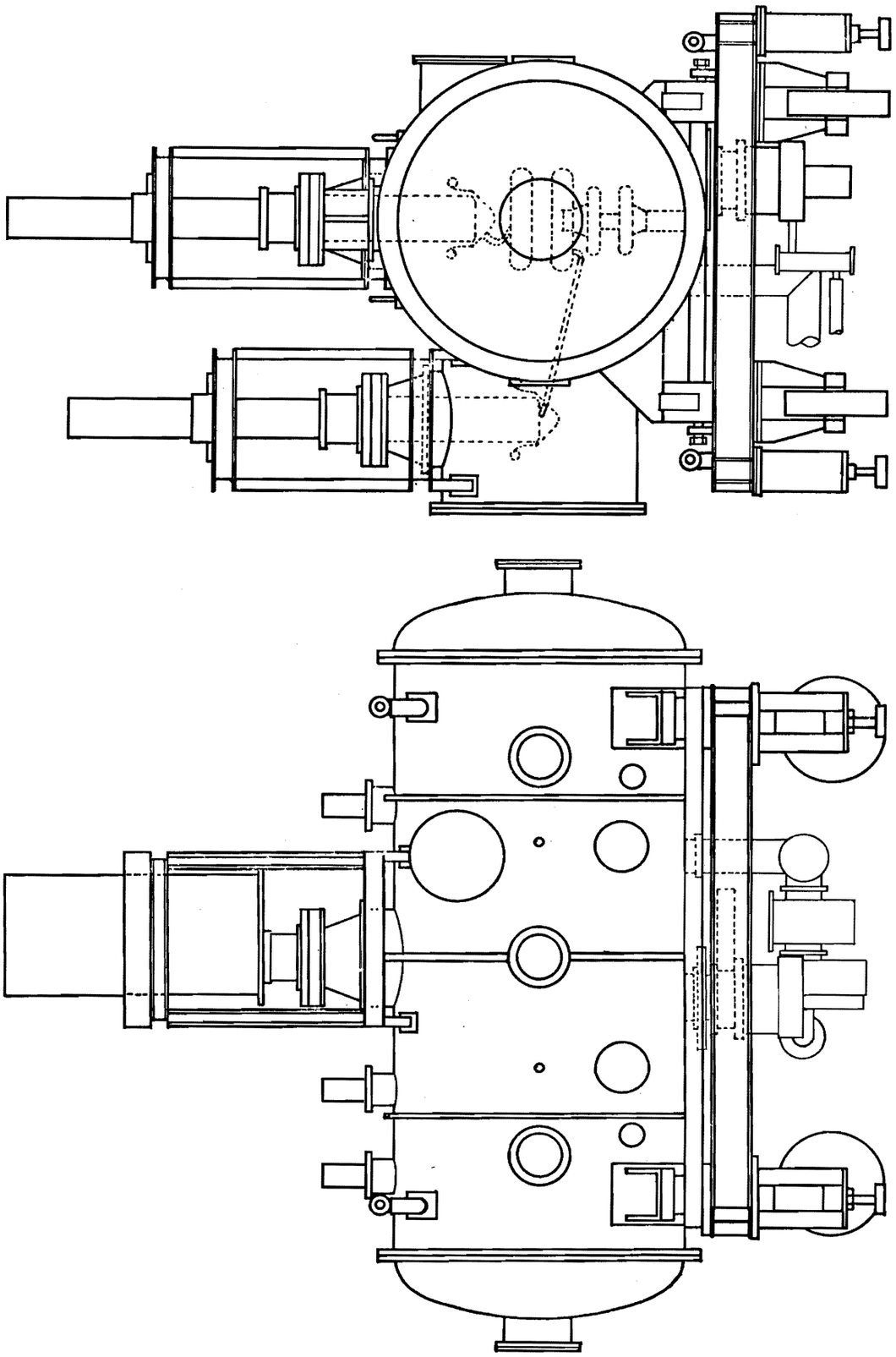

Fig. 14

Fig. 15

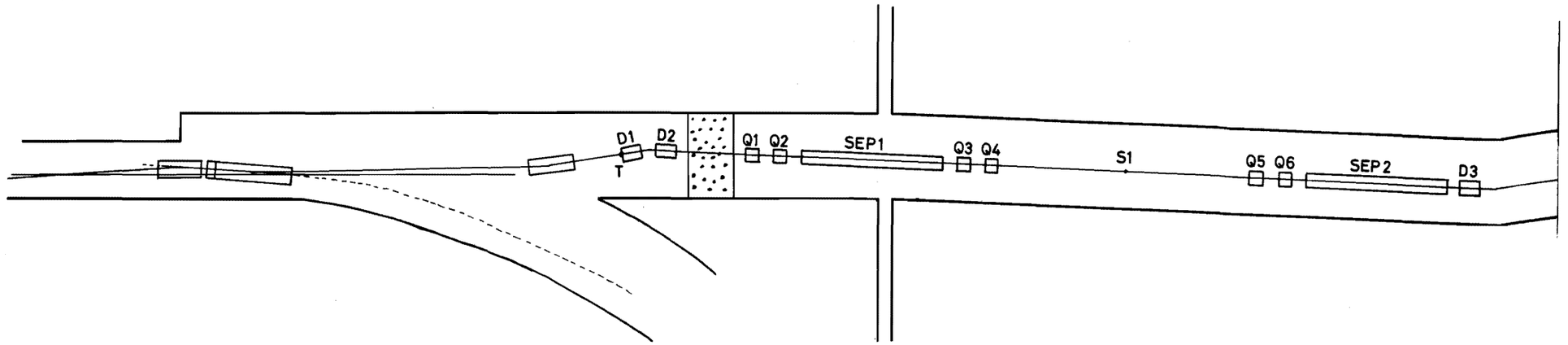

KEK K1 BEAM LINE

B1~B4 : Bending Magnet
Q1~Q10 : Quadrupole Magnet
S1,2 : Slit
SEP1,2 : Mass Separator

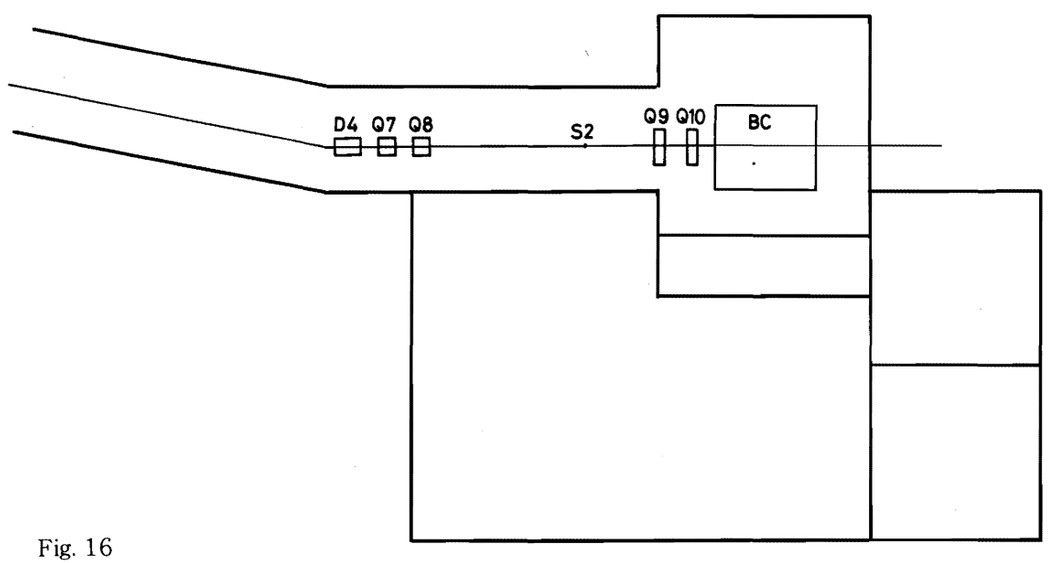

KEK BUBBLE
CHAMBER BLDG.

Fig. 16

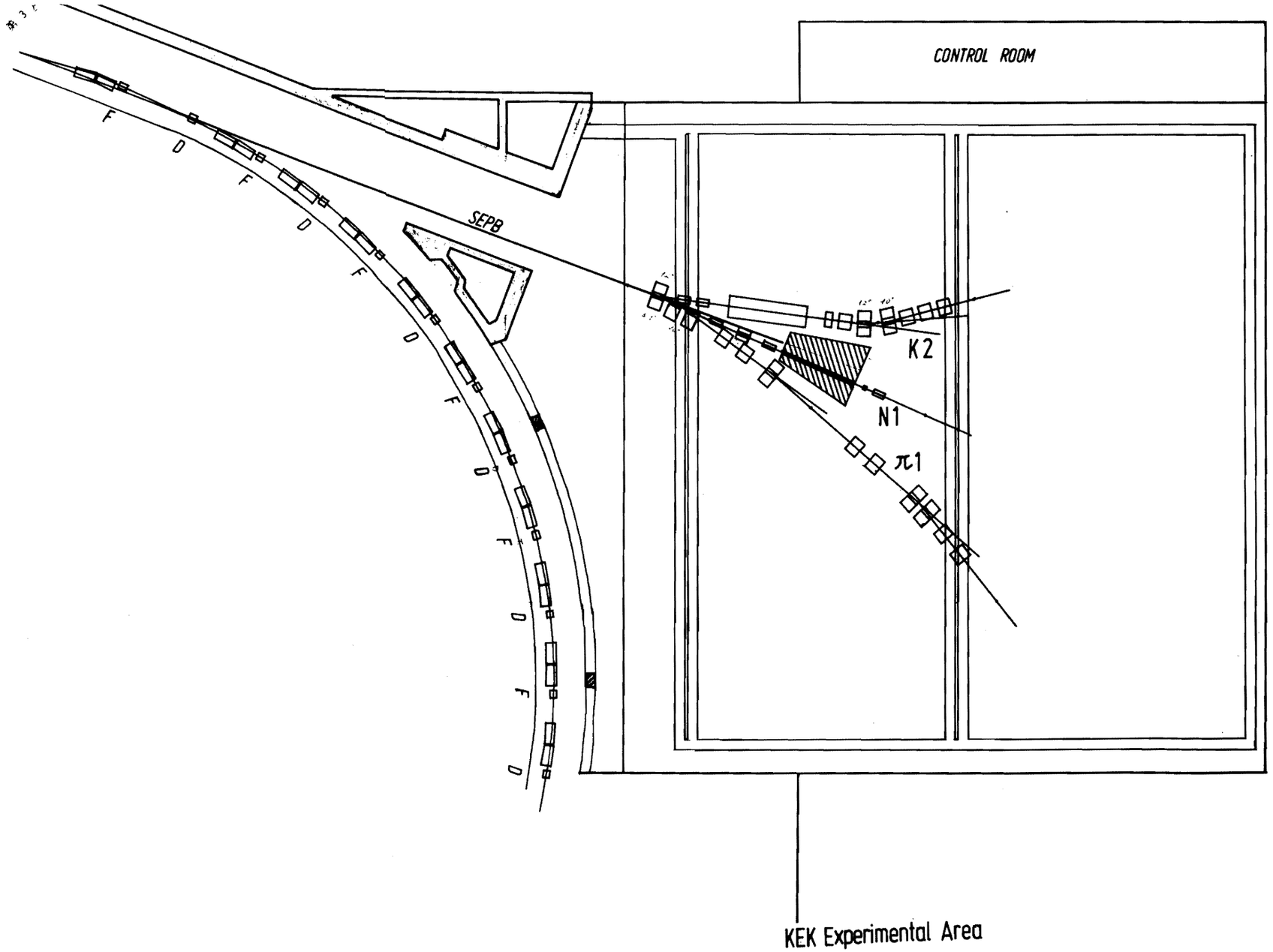

Fig. 17

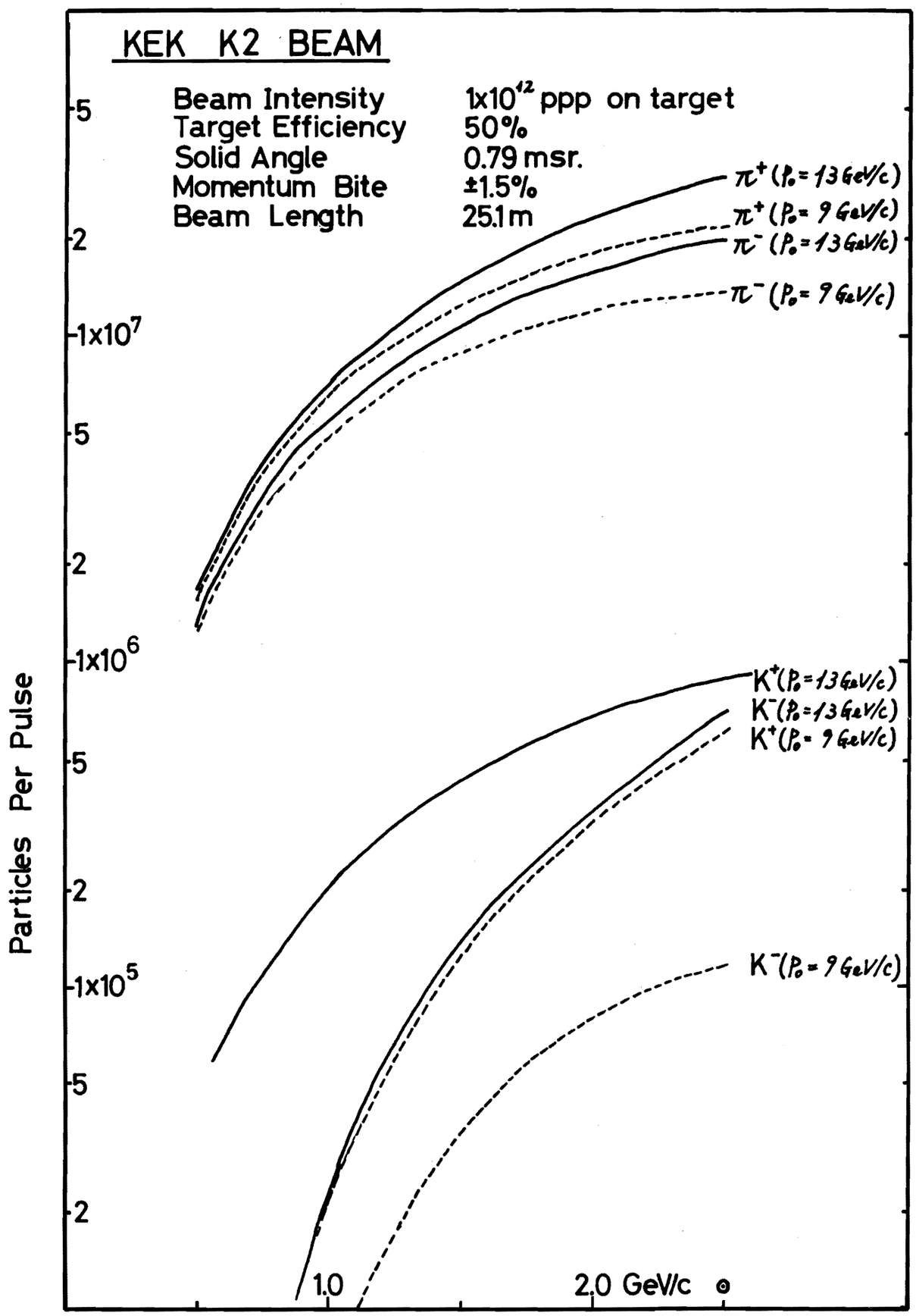
KEK K2 BEAM
Beam Intensity 1x10^12 ppp on target
Target Efficiency 50%
Solid Angle 0.79 msr.
Momentum Bite ±1.5%
Beam Length 25.1m
π+ (P0 = 13 GeV/c)
π+ (P0 = 9 GeV/c)
π- (P0 = 13 GeV/c)
π- (P0 = 9 GeV/c)
K+ (P0 = 13 GeV/c)
K- (P0 = 13 GeV/c)
K+ (P0 = 9 GeV/c)
K- (P0 = 9 GeV/c)
Particles Per Pulse
5
2
1x10^7
5
2
1x10^6
5
2
1x10^5
5
2
1.0
2.0 GeV/c

Fig. 18

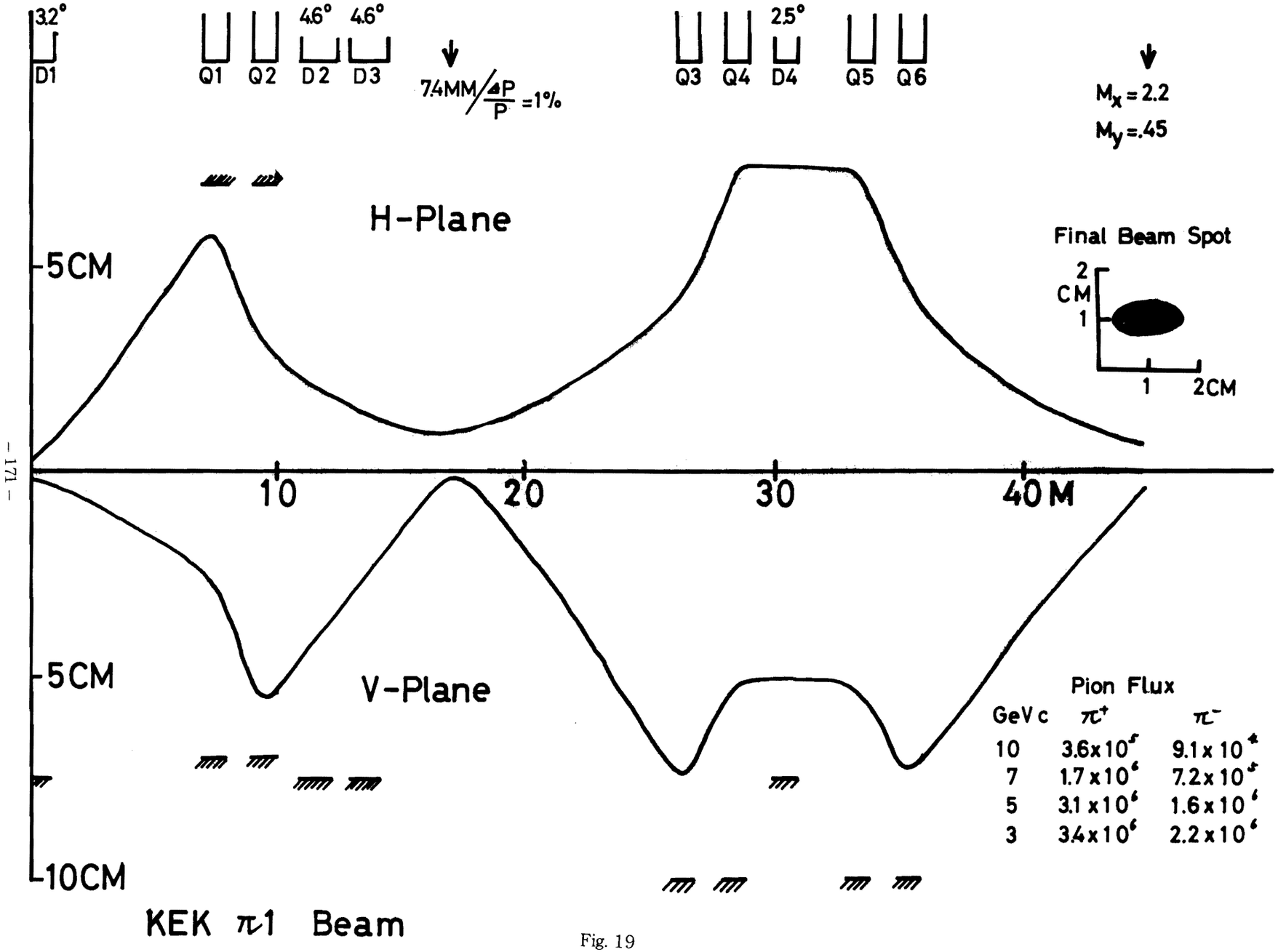
3.2°
D1
Q1
Q2
4.6°
D2
4.6°
D3
7.4MM/ΔP/P =1%
Q3
Q4
2.5°
D4
Q5
Q6
Mx = 2.2
My = .45
H-Plane
5CM
Final Beam Spot
2
CM
1
1
2CM
10
20
30
40 M
5CM
V-Plane
10CM
Pion Flux
GeV c
π+
π−
10
3.6x10⁶
9.1x10⁴
7
1.7x10⁶
7.2x10⁴
5
3.1x10⁶
1.6x10⁶
3
3.4x10⁶
2.2x10⁶
KEK π1 Beam

Fig. 19

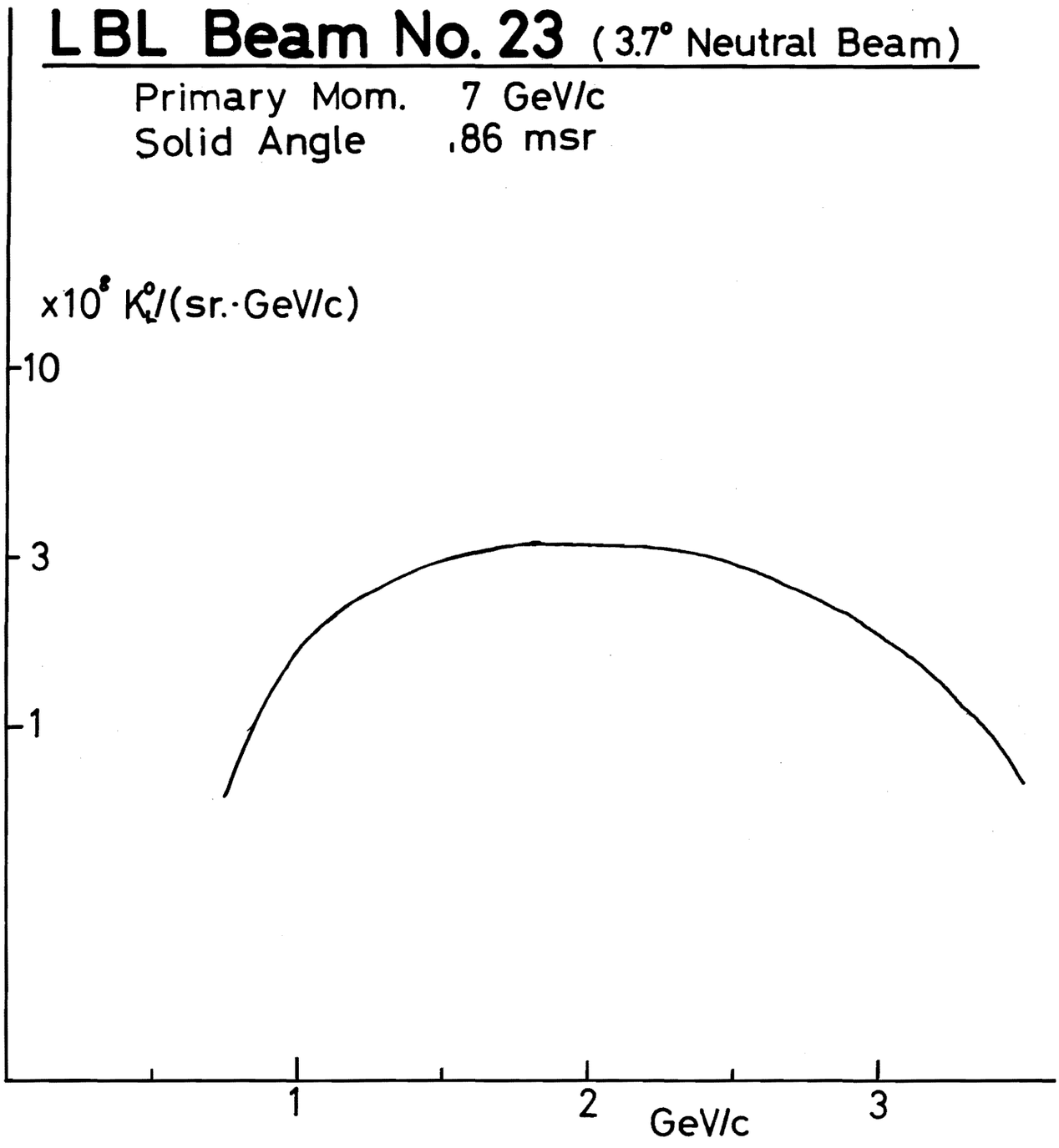
LBL Beam No. 23 (3.7° Neutral Beam)
Primary Mom. 7 GeV/c
Solid Angle .86 msr
x10⁶ K°L/(sr.·GeV/c)
10
3
1
1
2
3
GeV/c

Fig. 20

Particle Production Rate

(Experimental Data)

	Machine	Primary Momentum	Target	Secondary Particle	Production Angle	Momentum Range	Reference
1	CERN-PS	25 GeV	Al	$(K,^+ P, d)/\pi^+$	15.9°	2~5.3 GeV/c	V.T.Cocconi et al. PRL 5 ('60) 19
				$(K^-, P)/\pi^-$			
2	CERN-PS	25 GeV	Al	K^+/π^+	3° 6°		G. von Dardel, et al
				K^-/π^-	6°	5, 6, 8GeV/c	Roch. Conf ('60)
				$\bar{P}/\pi^-$	6°	6~16GeV/c	P. 837
				d/π^+		18GeV/c	
3	CERN-PS	24GeV	Al	K^+/K^-	8.5°	1.5GeV/c	L. Gilly et al
				$P/\bar{P}$	8.5°	3GeV/c	Roch Conf ('60)
				$d/\bar{d}$	8.5°	6GeV/c	P. 808
4	BNL-AGS	2.9GeV	H_2	$\pi^\pm$	0°, 17, 32°	0.2~2.0GeV/c	A.C.Melissinos etal PRL 7 ('61) 454
5	BNL-A6S	10-30GeV	Al, Be	$\pi^\pm$	4.75°, 9°, 13°	0.5~16GeV/c	W.F. Baker, et al
					20°		PRL 1 ('61) 101
				$K^+/\pi^+, K^-/\pi^-$	4.75°, 9°	1.25~16GeV/c	
				$\bar{P}/\pi^-$	13°, 20°		
6	BNL-AGS	30, 33GeV	Al, Be	$\pi^\pm, P, \bar{P}$	13.25°	0.1~5GeV/c	V.L. Fitch, et al.
				d, t, H_e^3	45°, 90°		PR 126 ('62) 1849
7	BNL-AGS	30GeV	Be, Al	P, $\bar{P}$, $\pi^\pm$	30°	1~3GeV/c	A, Schwarzschild, et al.
			St. St.	K^1, d, t			PR 129 ('63) 854
8	ANL-ZGS	12.5GeV	Be	$\pi^\pm, P, K^\pm$	2°~16°	1~13GeV/c	R.A.Lundy, et al.
							PRL 14 ('65) 504
9	CERN-PS	18, 8, 23.1GeV	Be, Pb	$\pi^\pm, K^\pm, P$	0.100mr	1~12GeV/c	D. Dekkers, et al
			H_2	$\bar{P}$			P.R. 131 ('65) B962
10	ANL-ZGS	12.5GeV	Be	$\pi^\pm$	15°	3, 4, 5GeV/c	J. G. Asbury, et al.
				π^+	12°		P.R. 178 ('69) 2086
11	ANL-ZGS	12.5GeV	Cu, Be	$\pi^\pm, K^\pm, P$	0-11.2°	.5~1.03 GeV/c	G.J. Marmer, et al.
				$\bar{P}$, d, t, H_e^3			P.R. 179 ('69) 1294

Decay Factor

			L=40 m			20 m	
	m (GeV)	$C\tau$ (m)	P=1 (GeV/c) 5	8	1	5	8
π^+	.140	7.81	.488	.866	.914	.698	.931	.956
$K^\pm$	.494	3.70	.00479	.344	.513	.0692	.586	.714
K^o_L	.498	16.14	.291	.781	.857	.540	.884	.926